*Pramana – J. Phys.* (2017) 88: 63
DOI 10.1007/s12043-017-1372-5



# The hydrodynamic description of pseudorapidity distributions at lower energies at BNL-RHIC

ZHI-JIN JIANG*, YAN HUANG, HAI-LI ZHANG and YU ZHANG

College of Science, University of Shanghai for Science and Technology, Shanghai 200093, China
*Corresponding author. E-mail: jzj265@163.com

MS received 3 June 2016; revised 3 December 2016; accepted 16 December 2016; published online 15 March 2017

**Abstract.** The hot and dense matter produced in nucleus–nucleus collisions is supposed to expand according to unified hydrodynamics, one of the few theoretical models that can be worked out exactly. The solution is then used to formulate the rapidity distribution of charged particles frozen out from the fluid on the space-like hypersurface with a fixed temperature, $T_{\mathrm{FO}}$. A comparison is made between the theoretical predictions and the experimental measurements carried out by PHOBOS Collaboration in the Relativistic Heavy Ion Collider (RHIC) at the Brookhaven National Laboratory (BNL) in different centrality Au–Au and Cu–Cu collisions at $\sqrt{s_{\mathrm{NN}}} = 19.6$ and 22.4 GeV, respectively. The theoretical results are in good accordance with experimental data.

**Keywords.** Unified hydrodynamics; charged particle; pseudorapidity distribution.

**PACS Nos 25.75.−q; 25.75.Ld; 24.10.Nz**

## 1. Introduction

Relativistic hydrodynamics, since its success in describing the elliptic flow and multiplicity production in nucleus–nucleus collisions [1–3], has now been widely taken as one of the best tools for understanding the spatiotemporal evolution of the matter created in collisions [4–14]. If the initial conditions and the equation of state are given, the evolution of fluid relies only on the local energy–momentum conservation and the assumption of local thermal equilibrium. From this point of view, hydrodynamics is simple and powerful. On the other hand, the initial conditions and the equation of state are not well known. Worse still is that the partial differential equations of relativistic hydrodynamics are highly non-linear and coupled. It is very hard to solve them analytically. From this point of view, hydrodynamics is tremendously complicated. This is the reason why from the time of Landau [15] till now what we can solve exactly is limited only to $1 + 1$ evolutions for perfect fluid with simple equation of state. $3 + 1$ expansions have few analytical discussions so far. The treatment of them usually resorts to numerical simulations. In numerical simulations, beside a powerful calculation system, sophisticated skills are also needed for avoiding instabilities in solving partial differential hydrodynamic equations. Furthermore, as the results come from a complicated non-transparent software package, the correlations between them and physical law are not direct and clear. On the contrary, the analytical methods, concerning the most essential and important elements affecting the physical phenomena via ideal assumptions, provide us with the most basic underlying law. In addition, the concise and explicit form of exact solution is unmatchable for numerical simulations. Hence, despite facing tremendous difficulties and being usually amenable for a certain special case, finding analytical solution of relativistic hydrodynamic equations is always our goal. It is an important field in high-energy physics.

The first exact analytical solution of $1 + 1$ hydrodynamics was given by Khalatnikov about 62 years ago [16]. This solution is for an accelerated system with the fluid being assumed as a massless and perfect fluid which is initially at rest. The result obtained is very unpleasant because it is presented in a rather implicit way. However, from this complicated solution, Landau managed to extract the rapidity distribution of the charged particles produced [17], which is in general

consistent with the observations made at BNL-RHIC [18–20].

The second exact analytical solution of 1+1-dimensional hydrodynamics was given by Hwa about 42 years ago [21]. This solution is for an accelerationless system with Lorentz-invariant initial condition. The result obtained in this way is simple and explicit. From this solution, Bjorken [22] was able to get a simple estimate for the initial energy density achieved in collisions from the final observables. This makes the energy density measurable in experiment. It is the first and till now the only formula being widely recognized as the one for estimating the energy density of matter created in collisions. Hence, it receives much attention. This is the reason why Hwa's theory is usually named as Hwa–Bjorken hydrodynamic model. However, as the free parameter in the formula has not been fixed properly, determination of the mentioned energy density is still an open problem. Moreover, the invariant rapidity distributions obtained from this model are at variance with experimental observations.

It is worth noting that a series of exact solutions of relativistic hydrodynamics has been found in recent years [23–27]. By generalizing Hwa–Bjorken in–out ansatz for fluid trajectories, Bialas *et al* [23] presented a family of exact solutions. The typical characteristic of this model is that it interpolates between Hwa–Bjorken picture and Landau one, and thus unifies these two famous hydrodynamic models as one. By taking advantage of the scheme of Khalatnikov potential, Beuf *et al* [24] solved analytically the hydrodynamic equations and gave a pack of simple exact solutions for a perfect fluid with linear equation of state. By taking into account the work done by the fluid elements on each other, Csörgő *et al* [25] generalized the Hwa–Bjorken model for an accelerationless system to the one for an accelerated system, and obtained a new class of exact analytical solutions of relativistic hydrodynamics.

In the present paper, by using unified hydrodynamics [23], we shall discuss the pseudorapidity distributions of charged particles produced in nucleus–nucleus collisions. A brief introduction to the exact solutions of this model is given in the following section. The solutions are then used in §3 to get the rapidity distributions. In §4, a comparison is made between the theoretical results and the experimental data [28] presented by PHOBOS Collaboration at BNL-RHIC in different centrality Au–Au and Cu–Cu collisions at $\sqrt{s_{\rm NN}} = 19.6$ and 22.4 GeV, respectively. The last section gives conclusions.

## 2. A brief introduction to the exact solutions of unified hydrodynamics

The main points of unified hydrodynamics are as follows:

(1) The motion of fluid obeys the equation

$$\frac{\partial T^{\mu\nu}}{\partial x^{\mu}} = 0, \tag{1}$$

where $x^{\mu} = (x^0, x^1, x^2, x^3) = (t, z, x, y)$ is the space–time 4-vector, $T^{\mu\nu}$ is the energy–momentum tensor, and for a perfect fluid

$$T^{\mu\nu} = (\varepsilon + p)u^{\mu}u^{\nu} - pg^{\mu\nu}, \tag{2}$$

$u^{\mu}$, $g^{\mu\nu} = \mathrm{diag}(1, -1, -1, -1)$, $\varepsilon$, and $p$ are the 4-velocity, metric tensor, energy density, and pressure, respectively. $\varepsilon$ and $p$ are related by the equation of state

$$p = c_{\rm s}^2\varepsilon, \tag{3}$$

where $c_{\rm s}$ is the speed of sound. Investigations have shown that, for heavy-ion collisions at BNL-RHIC energies, $c_{\rm s}$ takes a constant value of about 0.35 [29–32].

(2) Using eqs (2) and (3), and noting the light-cone components of 4-volicity

$$u_{\pm} = \mathrm{e}^{\pm y},$$

where $y$ is the ordinary rapidity of the fluid, the $1 + 1$ expansions of the fluid follow equations

$$\begin{aligned}
&\frac{\mathrm{e}^{2y}-1}{2}(c_{\rm s}^2+1)\partial_+ p + \mathrm{e}^{2y}(c_{\rm s}^2+1)p\partial_+ y \\
&\quad + \frac{1-\mathrm{e}^{-2y}}{2}(c_{\rm s}^2+1)\partial_- p + \mathrm{e}^{-2y}(c_{\rm s}^2+1)p\partial_- y \\
&\quad + c_{\rm s}^2(\partial_+ p - \partial_- p) = 0, \\
&\frac{\mathrm{e}^{2y}+1}{2}(c_{\rm s}^2+1)\partial_+ p + \mathrm{e}^{2y}(c_{\rm s}^2+1)p\partial_+ y \\
&\quad + \frac{1+\mathrm{e}^{-2y}}{2}(c_{\rm s}^2+1)\partial_- p - \mathrm{e}^{-2y}(c_{\rm s}^2+1)p\partial_- y \\
&\quad - c_{\rm s}^2(\partial_+ p + \partial_- p) = 0,
\end{aligned} \tag{4}$$

where $\partial_+$ and $\partial_-$ are the compact notations of partial derivatives with respect to light-cone coordinates $z_{\pm} = t \pm z = x^0 \pm x^1 = \tau\mathrm{e}^{\pm\eta_{\rm s}}$, $\tau = \sqrt{z_+ z_-}$ is the proper

time, and $\eta_S = 1/2 \ln(z_+ z_-)$ is the space–time rapidity of the fluid. The solutions of the above equations are

$$c_s^2 \partial_+ \ln p = -\frac{(1+c_s^2)^2}{2}\partial_+ y - \frac{1-c_s^4}{2} e^{-2y}\partial_- y,$$
$$c_s^2 \partial_- \ln p = \frac{(1+c_s^2)^2}{2}\partial_- y + \frac{1-c_s^4}{2} e^{2y}\partial_+ y. \quad (5)$$

(3) The key ingredient of unified hydrodynamics is that it generalizes the relation between $y$ and $\eta_S$ via

$$2y = \ln u_+ - \ln u_- = \ln F_+(z_+) - \ln F_-(z_-), \quad (6)$$

where $F_\pm(z_\pm)$ are *a priori* arbitrary functions. When

$$F_\pm(z_\pm) = z_\pm, \quad (7)$$

eq. (6) reduces to $y = \eta_S$, returning to the boost-invariant picture of Hwa–Bjorken. Otherwise, eq. (6) describes the non-boost-invariant geometry of Landau. Accordingly, eq. (6) unifies the Hwa–Bjorken and Landau hydrodynamics. It paves a way between these two models.

(4) Inserting eq. (6) into eq. (5), it turns into

$$c_s^2 \partial_+ \ln p = -\frac{(1+c_s^2)^2}{4}\frac{f_+'}{f_+} + \frac{1-c_s^4}{4}\frac{f_-'}{f_+},$$
$$c_s^2 \partial_- \ln p = -\frac{(1+c_s^2)^2}{4}\frac{f_-'}{f_-} + \frac{1-c_s^4}{4}\frac{f_+'}{f_-}, \quad (8)$$

where

$$f_\pm = \frac{F_\pm}{H}, \quad z_\pm = h\int_0^{f_\pm} \frac{\mathrm{d}x}{\sqrt{\ln x}}, \quad (9)$$

$H$ and $h$ are two arbitrary constants. From eq. (8), we get the solution of unified hydrodynamics [23]

$$s = s_0 \left(\frac{p}{p_0}\right)^{\frac{1}{1+c_s^2}}$$
$$= s_0 \exp\left[-\frac{1+c_s^2}{4c_s^2}(l_+^2 + l_-^2) + \frac{1-c_s^2}{2c_s^2} l_+ l_-\right]$$
$$= s_0 \exp(-\theta/c_s^2), \quad (10)$$

where $s$ is the entropy density of the fluid, and

$$l_\pm(z_\pm) = \sqrt{\ln f_\pm} \quad (11)$$

$$y(z_+, z_-) = \frac{1}{2}(l_+^2 - l_-^2) \quad (12)$$

$$\theta = \ln\left(\frac{T_0}{T}\right) = \frac{1+c_s^2}{4}(l_+^2 + l_-^2) - \frac{1-c_s^2}{2} l_+ l_- \quad (13)$$

$T$ is the temperature of the fluid, and $T_0$ is its initial scale.

## 3. The rapidity distributions of the produced charged particles

From eq. (10), we get the rapidity distribution of charged particles produced in high-energy heavy-ion collisions. To this end, we first evaluate the entropy distribution of the fluid at the freeze-out temperature $T_{FO} = T_0 e^{-\theta_{FO}}$ as a function of rapidity $y$. The entropy distribution at freeze-out temperature is defined as the amount of entropy flowing through the space-like hypersurface with a fixed temperature of $T_{FO}$ in a unit rapidity interval. It has the form as [23]

$$\frac{\mathrm{d}S}{\mathrm{d}y} = s\frac{u^\mu \mathrm{d}\lambda_\mu}{\mathrm{d}y}\bigg|_{FO} = s u^\mu n_\mu \frac{\mathrm{d}\lambda}{\mathrm{d}y}\bigg|_{FO}, \quad (14)$$

where $n^\mu$ is the four-dimensional unit vector, $\mathrm{d}\lambda$ is the space-like slab element along the hypersurface, defined as $\mathrm{d}\lambda^\mu = \mathrm{d}\lambda n^\mu$, meeting

$$(\mathrm{d}\lambda)^2 = \mathrm{d}\lambda^\mu \mathrm{d}\lambda_\mu = -\mathrm{d}z^+ \mathrm{d}z^-, \quad (15)$$

with the minus sign coming from the space-like characteristic of $\mathrm{d}\lambda$.

Consider a hypersurface

$$\phi(z_+, z_-) = C,$$

where $C$ is a constant. Then

$$\mathrm{d}\lambda = \sqrt{-\mathrm{d}z_+ \mathrm{d}z_-} = \mathrm{d}z_- \sqrt{\frac{\partial_-\phi}{\partial_+\phi}} = \mathrm{d}z_+ \sqrt{\frac{\partial_+\phi}{\partial_-\phi}}.$$

Thus, the expression on the right-hand side of eq. (14) is

$$u^\mu n_\mu \mathrm{d}\lambda = \frac{1}{2}(u_+ n_- + u_- n_+)\mathrm{d}\lambda$$
$$= \frac{1}{2}(u_+\partial_+\phi + u_-\partial_-\phi)\frac{\mathrm{d}z_-}{\partial_+\phi}$$
$$= \frac{1}{2}(u_+\partial_+\phi + u_-\partial_-\phi)\frac{\mathrm{d}z_+}{\partial_-\phi}. \quad (16)$$

Furthermore, from eqs (9) and (11),

$$\mathrm{d}z_\pm = \frac{h}{l_\pm}\exp(l_\pm^2)\mathrm{d}l_\pm^2 = \pm\frac{2h\partial_\mp\phi}{\partial_+\phi l_-\exp(-l_-^2)+\partial_-\phi l_+\exp(-l_+^2)}\mathrm{d}y. \quad (17)$$

From the above two equations, eq. (14) becomes

$$\frac{\mathrm{d}S}{\mathrm{d}y} = s\mathrm{e}^{\frac{1}{2}(l_+^2+l_-^2)}\frac{\partial_+\phi\mathrm{e}^y+\partial_-\phi\mathrm{e}^{-y}}{\partial_+\phi l_-\mathrm{e}^y+\partial_-\phi l_+\mathrm{e}^{-y}}\bigg|_{\mathrm{FO}}. \quad (18)$$

In the above equation, the right-hand side is evaluated at the hypersurface with temperature $T_{\mathrm{FO}}$. From eq. (13), this hypersurface can be taken as

$$\phi(z_+,z_-) = \frac{\theta_{\mathrm{FO}}}{c_\mathrm{s}^2} = \frac{1}{c_\mathrm{s}^2}\ln\left(\frac{T_0}{T_{\mathrm{FO}}}\right) = \frac{1+c_\mathrm{s}^2}{4c_\mathrm{s}^2}(l_+^2+l_-^2) - \frac{1-c_\mathrm{s}^2}{2c_\mathrm{s}^2}l_+l_- = C.$$

Hence

$$\partial_+\phi = \frac{(1+c_\mathrm{s}^2)l_+-(1-c_\mathrm{s}^2)l_-}{4c_\mathrm{s}^2h\mathrm{e}^{l_+^2}},$$

$$\partial_-\phi = \frac{(1+c_\mathrm{s}^2)l_--(1-c_\mathrm{s}^2)l_+}{4c_\mathrm{s}^2h\mathrm{e}^{l_-^2}}. \quad (19)$$

Inserting eqs (10) and (19) into eq. (18), it becomes

$$\frac{\mathrm{d}S}{\mathrm{d}y} = s_0\mathrm{e}^{-\frac{1}{4c_\mathrm{s}^2}(1-c_\mathrm{s}^2)(l_+-l_-)^2} \times\frac{c_\mathrm{s}^2(l_++l_-)}{(1+c_\mathrm{s}^2)l_+l_- - \frac{1-c_\mathrm{s}^2}{2}(l_+^2+l_-^2)}\bigg|_{\mathrm{FO}}. \quad (20)$$

Moreover, from eqs (12) and (13)

$$l_-^2 = \frac{1+c_\mathrm{s}^2}{2c_\mathrm{s}^2}\theta - y + \frac{1-c_\mathrm{s}^2}{2c_\mathrm{s}^2}\sqrt{\theta^2-y^2c_\mathrm{s}^2},$$

$$l_+^2 = 2y + l_-^2,$$

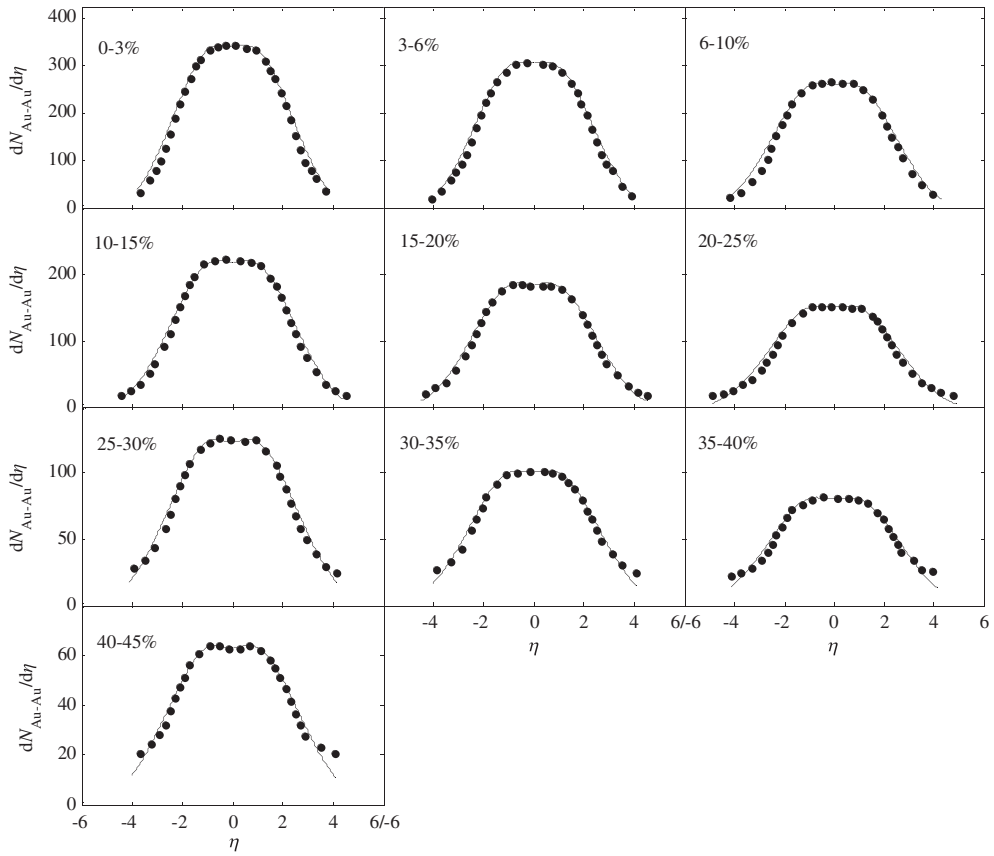


**Figure 1.** The pseudorapidity distributions of the produced charged particles in different centrality Au–Au collisions at $\sqrt{s_{\mathrm{NN}}} = 19.6$ GeV. The solid circles are the experimental measurements [28] and the solid curves are the results from unified hydrodynamics of eq. (21).

allowing the factors in eq. (20) to be expressed in terms of rapidity $y$ as

$$\frac{1}{4c_s^2}(1-c_s^2)(l_+-l_-)^2 = \frac{1-c_s^2}{2c_s^2}\left(\theta-\sqrt{\theta^2-y^2c_s^2}\right),$$

$$l_+ + l_- = \sqrt{2}y\frac{1}{\left(\theta-\sqrt{\theta^2-y^2c_s^2}\right)^{1/2}},$$

$$(1+c_s^2)l_+l_- - \frac{1-c_s^2}{2}(l_+^2+l_-^2) = 2\sqrt{\theta^2-y^2c_s^2}.$$

Substituting them into eq. (20), we finally obtain [23]

$$\frac{\mathrm{d}S}{\mathrm{d}y} = \frac{s_0c_s^2}{\sqrt{2}}\mathrm{e}^{-\frac{1-c_s^2}{2c_s^2}\left(\theta_{\mathrm{FO}}-\sqrt{\theta_{\mathrm{FO}}^2-y^2c_s^2}\right)} \times\frac{y}{\left[\left(\theta_{\mathrm{FO}}-\sqrt{\theta_{\mathrm{FO}}^2-y^2c_s^2}\right)\left(\theta_{\mathrm{FO}}^2-y^2c_s^2\right)\right]^{1/2}},$$

where $\theta_{\mathrm{FO}} = \ln(T_0/T_{\mathrm{FO}})$. It is related to the initial temperature of the fluid and is therefore dependent on the incident energy and collision centrality. Its specific values can be determined by comparing the theoretical predictions with the experimental data.

As entropy is proportional to the number of produced charged particles, we obtain the rapidity distribution

$$\frac{\mathrm{d}N(b,\sqrt{s_{\mathrm{NN}}},y)}{\mathrm{d}y} = C(b,\sqrt{s_{\mathrm{NN}}})\mathrm{e}^{-\frac{1-c_s^2}{2c_s^2}\left(\theta_{\mathrm{FO}}-\sqrt{\theta_{\mathrm{FO}}^2-y^2c_s^2}\right)} \times\frac{y}{\left[\left(\theta_{\mathrm{FO}}-\sqrt{\theta_{\mathrm{FO}}^2-y^2c_s^2}\right)\left(\theta_{\mathrm{FO}}^2-y^2c_s^2\right)\right]^{1/2}}, \quad (21)$$

where $C(b,\sqrt{s_{\mathrm{NN}}})$, independent of rapidity $y$, is an overall normalization constant, $b$ is the impact parameter, and $\sqrt{s_{\mathrm{NN}}}$ is the center-of-mass energy per pair of nucleons.

In nucleus–nucleus collisions at high energy, owing to the violent collisions and intense compression along colliding or longitudinal axis, the pressure gradient is very large in this direction. This large pressure gradient plays a dominant role in later fluid expansions. In

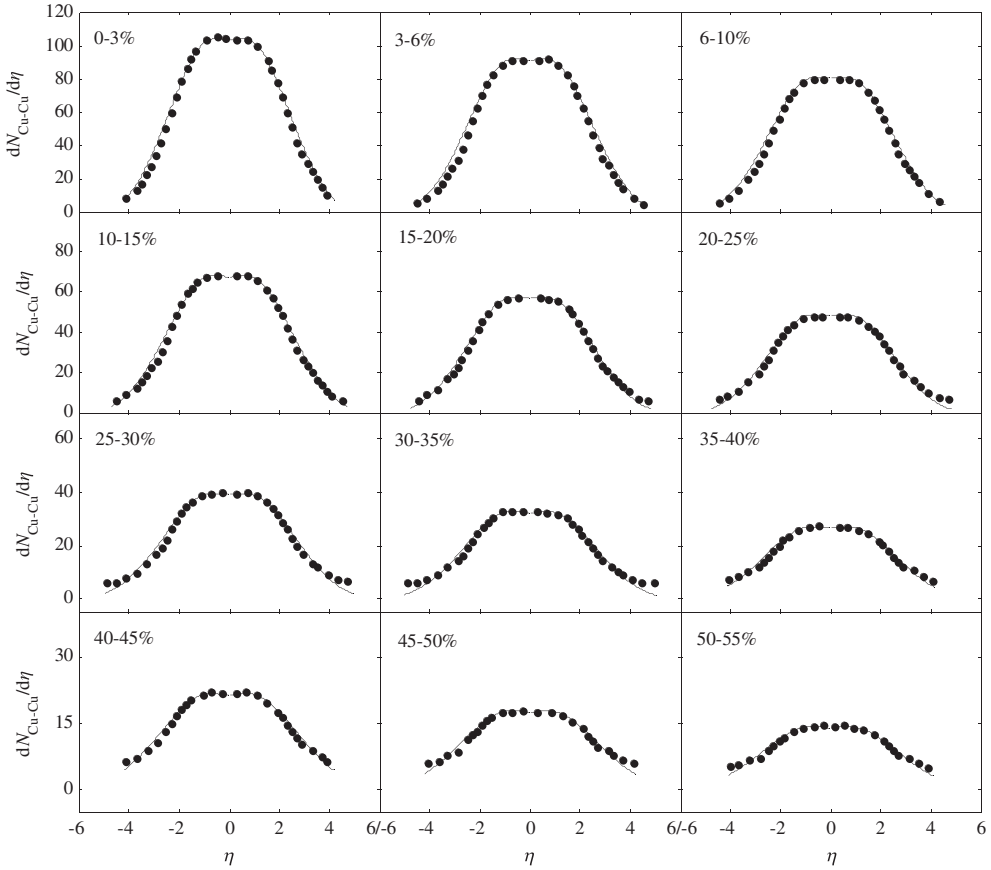


**Figure 2.** The pseudorapidity distributions of the produced charged particles in different centrality Cu–Cu collisions at $\sqrt{s_{\mathrm{NN}}} = 22.4$ GeV. The solid dots are the experimental measurements [28] and the solid curves are the results from unified hydrodynamics of eq. (21).

contrast, the effect of thermal movements of particles in fluid is negligibly small. Hence, as in other papers [4,5], the thermal distribution is not taken into account in this paper.

## 4. A comparison between theoretical results and experimental data

From eq. (21), we get the pseudorapidity distribution through the relation [33]

$$\frac{\mathrm{d}N(b,\sqrt{s_{\mathrm{NN}}},\eta)}{\mathrm{d}\eta}=\sqrt{1-\frac{m^2}{m_{\mathrm{T}}^2\cosh^2 y}}\,\frac{\mathrm{d}N(b,\sqrt{s_{\mathrm{NN}}},y)}{\mathrm{d}y}, \tag{22}$$

$$y=\frac{1}{2}\ln\left[\frac{\sqrt{p_{\mathrm{T}}^2\cosh^2\eta+m^2}+p_{\mathrm{T}}\sinh\eta}{\sqrt{p_{\mathrm{T}}^2\cosh^2\eta+m^2}-p_{\mathrm{T}}\sinh\eta}\right], \tag{23}$$

where $p_{\mathrm{T}}$ is the transverse momentum, $m_{\mathrm{T}}=\sqrt{m^2+p_{\mathrm{T}}^2}$ is the transverse mass.

Substituting eq. (21) into (22), we get the pseudorapidity distributions of produced charged particles. Figures 1 and 2 show such distributions in different centrality Au–Au and Cu–Cu collisions at $\sqrt{s_{\mathrm{NN}}}=19.6$ and 22.4 GeV, respectively. The solid circles in the figures are the experimental measurements [28]. The solid curves are the results obtained from unified hydrodynamics of eq. (21). It can be seen that the theoretical results are in good agreement with experimental measurements.

In calculations, the parameter $\theta_{\mathrm{FO}}$ in eq. (21) takes the values as listed in table 1. It can be seen that $\theta_{\mathrm{FO}}$ increases with centrality cuts and incident energies. It should, since $\theta_{\mathrm{FO}}$ in eq. (21) determines the widths of distributions, which increase with centrality cuts and incident energies (see figures 1 and 2).

In order to see the sensitivity of $c_{\mathrm{s}}$ to the results, figure 3 shows the pseudorapidity distributions of charged particles in 0–3% centrality Au–Au collisions at $\sqrt{s_{\mathrm{NN}}}=19.6$ GeV for three different values of $c_{\mathrm{s}}=0.35, 0.33$ and 0.31, corresponding to solid, dotted and dashed curve, respectively. Except for $c_{\mathrm{s}}$, the other parameters in eq. (21) are the same as those used in figure 1. It can be seen that the distributions in the mid-rapidity region are more sensitive to $c_{\mathrm{s}}$, and the height of the mid-platform increases with decreasing $c_{\mathrm{s}}$.

**Table 1.** The fitting values of the parameter $\theta_{\mathrm{FO}}$ in eq. (21) in different centrality Au–Au and Cu–Cu collisions at $\sqrt{s_{\mathrm{NN}}}=19.6$ and 22.4 GeV, respectively.

| Centrality cut (%) | 0–3 | 3–6 | 6–10 | 10–15 | 15–20 | 20–25 | 25–30 | 30–35 | 35–40 | 40–45 | 45–50 | 50–55 |
|---|---|---|---|---|---|---|---|---|---|---|---|---|
| $\theta_{\mathrm{FO}}$(Au–Au) | 1.35 | 1.44 | 1.53 | 1.60 | 1.65 | 1.72 | 1.74 | 1.77 | 1.81 | 1.84 | – | – |
| $\theta_{\mathrm{FO}}$(Cu–Cu) | 1.45 | 1.57 | 1.60 | 1.64 | 1.70 | 1.77 | 1.84 | 1.88 | 1.91 | 1.96 | 2.01 | 2.06 |

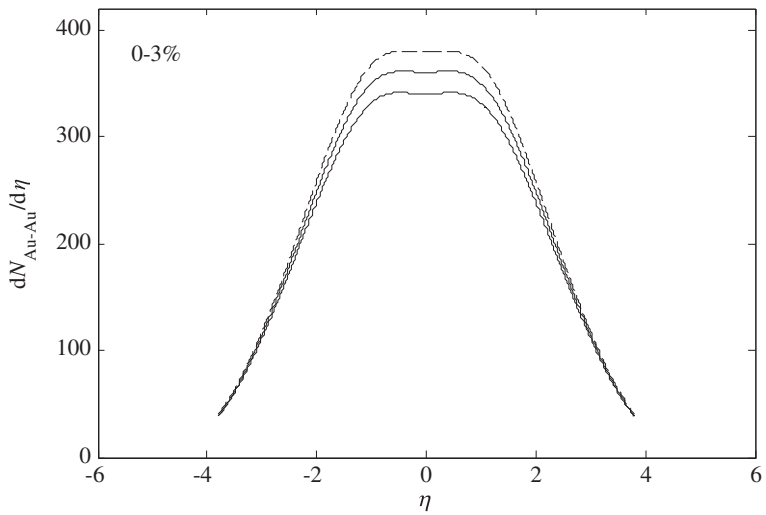


**Figure 3.** The $c_{\mathrm{s}}$ dependence of pseudorapidity distributions of the produced charged particles in 0–3% centrality Au–Au collisions at $\sqrt{s_{\mathrm{NN}}}=19.6$ GeV. The solid, dotted and dashed curves correspond to $c_{\mathrm{s}}=0.35, 0.33$ and 0.31, respectively.

Here, we would like to point out that due to the poor transparency of participants at lower RHIC energies, the mid-rapidity region is in fact rich in baryons [34]. However, compared with the large yield of charged particles frozen out from the fluid in this central rapidity region, the net baryon number is very small. The effect of baryons is totally hidden by that of charged particles resulted from fluid. In other words, the contribution of baryons is consolidated into that of frozen-out charged particles by modulating the overall normalization constant $C$ in eq. (21) which is currently indeterminable in both theory and experiment.

## 5. Conclusions

By generalizing the relation between ordinary rapidity $y$ and space–time rapidity $\eta_S$, two famous hydrodynamic models, Hwa–Bjorken and Landau, come together in the context of unified hydrodynamics. In linear equation of state, this hydrodynamics can be solved analytically and the solution can be used to derive rapidity distributions of charged particles frozen out from the fluid at the space-like hypersurface with the fixed temperature $T_{FO}$. This fulfils the connection between theoretical results and experimental measurements. In the derived formula, there are two parameters $c_s$ and $\theta_{FO}=\ln(T_0/T_{FO})$. $c_s$ takes the value from other investigations and $\theta_{FO}$ is fixed by tuning the theoretical results with experimental data. On comparing with experimental measurements performed by PHOBOS Collaboration at BNL-RHIC in different centrality Au–Au and Cu–Cu collisions at $\sqrt{s_{NN}} = 19.6$ and 22.4 GeV, respectively, we can see that the theoretical results are consistent with the experimental data.

In our previous work [8], we successfully used the evolution-dominated hydrodynamics in dealing with the same experimental data. That model differs from the present one in just one aspect: use of different initial conditions. The former supposes that the fluid is initially at rest. The latter, however, differs from this via relation (6). Different initial conditions lead to different solution methods and results of relativistic hydrodynamic equations. However, both solutions contain the same parameter $\theta_{FO}$. Comparing the values of $\theta_{FO}$ given in table 1 with those used in ref. [8], we can find that the values of the former are generally greater than those of the latter.

The existing studies show that both evolution-dominated and unified hydrodynamic models can give an equally proper description to the mentioned experimental observations. Then the question arises: which model is more reasonable? A conclusion can be drawn only after further experimental or theoretical researches. Only after the free parameter such as $\theta_{FO}$ in models is determined in experiment or theory can the answer become clear. In the absence of further experimental or theoretical evidences, each theoretical model might be potentially a good one if it is not contradicting the currently available experimental data.

## Acknowledgements

This work is partly supported by the Shanghai Key Lab of Modern Optical System.

## References

[1] PHENIX Collaboration: S S Adler *et al*, *Phys. Rev. Lett.* **91**, 182301 (2003)
[2] ALICE Collaboration: K Aamodt *et al*, *Phys. Rev. Lett.* **107**, 032301 (2011)
[3] CMS Collaboration: S Chatrchyan *et al*, *Phys. Rev. C* **87**, 014902 (2013)
[4] C Y Wong, *Phys. Rev. C* **78**, 054902 (2008)
[5] P Steinberg, *Nucl. Phys. A* **752**, 423 (2005)
[6] D K Srivastava, J E Alam, S Chakrabarty, B Sinha and S Raha, *Ann. Phys.* **228**, 104 (1993)
[7] Z J Jiang, Q G Li and H L Zhang, *Phys. Rev. C* **87**, 044902 (2013)
[8] Z J Jiang, H L Zhang, J Wang, K Ma and L M Cai, *Chin. J. Phys.* **52**, 1676 (2014)
[9] C Gale, S Jeon and B Schenke, *Int. J. Mod. Phys. A* **28**, 1340011 (2013)
[10] E K G Sarkisyan and A S Sakharov, *Eur. Phys. J. C* **70**, 533 (2010)
[11] G S Denicol, U Heinz, M Martinez, J Noronha and M Strickland, *Phys. Rev. Lett.* **113**, 202301 (2014)
[12] K Werner, M Bleicher, B Guiot, I Karpenko and T Pierog, *Phys. Rev. Lett.* **112**, 232301 (2014)
[13] Z J Jiang, K Ma, H L Zhang and L M Cai, *Chin. Phys. C* **38**, 084103 (2014)
[14] Z W Wang, Z J Jiang and Y S Zhang, *J. Univ. Shanghai Sci. Technol.* **31**, 322 (2009) (in Chinese)
[15] L D Landau, *Izv. Akad. Nauk SSSR* **17**, 51 (1953) (in Russian)
[16] I M Khalatnikov, *J. Exp. Theor. Phys.* **27**, 529 (1954) (in Russian)
[17] S Z Belenkij and L D Landau, *Nuovo Cimento Suppl.* **3**, 15 (1956)
[18] BRAHMS Collaboration: M Murray, *J. Phys. G: Nucl. Part. Phys.* **30**, 667 (2004)
[19] BRAHMS Collaboration: M Murray, *J. Phys. G: Nucl. Part. Phys.* **35**, 044015 (2008)
[20] BRAHMS Collaboration: I G Bearden *et al*, *Phys. Rev. Lett.* **94**, 162301 (2005)
[21] R C Hwa, *Phys. Rev. D* **10**, 2260 (1974)
[22] J D Bjorken, *Phys. Rev. D* **27**, 140 (1983)
[23] A Bialas, R A Janik and R Peschanski, *Phys. Rev. C* **76**, 054901 (2007)
[24] G Beuf, R Peschanski and E N Saridakis, *Phys. Rev. C* **78**, 064909 (2008)

[25] T Csörgő, M I Nagy and M Csanád, *Phys. Lett. B* **663**, 306 (2008)
[26] M S Borshch and V I Zhdanov, *SIGMA* **3**, 116 (2007)
[27] M Csanád, M I Nagy and S Lökös, *Eur. Phys. J. A* **48**, 173 (2012)
[28] PHOBOS Collaboration: B Alver *et al*, *Phys. Rev. C* **83**, 024913 (2011)
[29] PHENIX Collaboration: A Adare *et al*, *Phys. Rev. Lett.* **98**, 162301 (2007)
[30] N Armesto *et al*, *J. Phys. G: Nucl. Part. Phys.* **35**, 054001 (2008)
[31] T Mizoguchi, H Miyazawa and M Biyajima, *Eur. Phys. J. A* **40**, 99 (2009)
[32] S Borsányi, G Endrődi, Z Fodor, A Jakovác, S D Katz, S Krieg, C Ratti and K K Szabó, *J. High Energy Phys.* **77**, 1 (2010)
[33] C Y Wong, *Introduction to high energy heavy ion collisions* (Press of Harbin Technology University, Harbin, China, 2002) p. 23 (in Chinese); English edition (World Scientific, Singapore, 1994) p. 25
[34] BRAHMS Collaboration: I G Bearden *et al*, *Phys. Rev. Lett.* **93**, 102301 (2004)